

Effects of the Au/CdTe back contact on *IV* and *CV* characteristics of Au/CdTe/CdS/TCO solar cells

Alex Niemegeers^{a)} and Marc Burgelman

Department of Electronics and Information Systems (ELIS), University of Gent, B9000 Gent, Belgium

(Received 18 September 1996; accepted for publication 17 December 1996)

A simple analytical theory is presented to explain the measured roll over and cross over behaviour of the *IV* characteristics of thin film CdTe solar cells. It involves a classical description of the CdS/CdTe junction and the CdTe/back contact structure and is extended with a new description of minority carrier current in the CdTe contact region. This extension is crucial in describing the light dependence of the forward *IV* curves, and hence cross over. The same model also explains the measured *CV* curves. It is shown that analysis of the capacitance measurement can yield additional information about the doping density of CdTe in the vicinity of the contact. A relationship between the fill factor of the solar cell and the barrier height of the back contact is derived; this relation is useful as a new, practical criterion for the quality of the back contact. The results of this simple analytical model are confirmed by full numerical calculations of the dc and ac characteristics.

© 1997 American Institute of Physics. [S0021-8979(97)08606-4]

I. INTRODUCTION

Polycrystalline thin film CdTe solar cells are one of the important candidates for large scale photovoltaic applications. In the recent past, efficiencies have improved substantially. One of the major technological issues is the processing of a good back contact on CdTe.^{1,2} This paper discusses in detail the effects of a back contact barrier on current voltage (*IV*) and capacitance voltage (*CV*) measurements. Among these effects, the roll over of the *IV* curves (current saturation at high forward bias) is well understood.³ Cross over (dark and illuminated *IV* curves intersect) and the behaviour of the capacitance-voltage curves are less understood. A new, simple model is presented here to explain the cross over in CdTe/CdS solar cells, and a relationship between the back contact barrier height and the fill factor is derived. With this relationship, a useful definition of a “good” back contact is formulated. Also the peculiar behaviour of the capacitance-voltage curve is explained. This simple model, explaining roll over, cross over, fill factor loss and capacitance-voltage behaviour, is worked out in Section II.

This theory is applied to the Au/CdTe contact in Au/CdTe/CdS/TCO solar cell structures processed by ANTEC, Germany,⁴ and measured in Gent (Section III). It is shown that the transport of majority carriers through the back contact is limited by drift and diffusion rather than by thermionic emission. The barrier height as well as the CdTe acceptor concentration in the vicinity of the contact are deduced from *IV* and *CV* measurements.

To conclude, *IV* and *CV* measurements are compared with some fully numerical calculations, carried out by the program SCAPS-1D, developed in Gent⁵ (Section IV).

II. THEORY

Figure 1 shows the band diagram of a Au/p-CdTe/ n^+ -CdS junction with a back contact Schottky barrier, under

forward bias and in the dark. The contact barrier height $q\Phi_b$ is defined as the difference between the equilibrium Fermi level and the top of the valence band at the metal surface: $E_F - E_v(0)$. When a forward bias V is applied to the device (Figure 1), a part V_j of the voltage drops over the junction: $qV_j = E_{Fn}(L) - E_{Fp}(L_c)$. Since the back contact is not perfectly ohmic, a part V_c of the applied bias will drop over the back contact: $qV_c = E_{Fp}(L_c) - E_{Fp}(0)$. Excluding other sources of series resistance, we have:

$$V = V_c + V_j. \quad (1)$$

In the following, we will not concentrate on the detailed junction transport mechanisms, and the junction current J_j will be approximated by:

$$J_j = J_p(L_c) = J_s(e^{qV_j/nkT} - 1) - J_L, \quad (2)$$

where $J_p(x)$ stands for the hole current at position x . The current J_s denotes the dark saturation current of the CdS/CdTe junction, n the diode ideality factor and J_L the light current, generated in the CdTe layer between $x = L_c$ and $x = L_{CdTe}$.

The holes which recombine in the junction region are supplied by the back contact. From standard theory,^{6,7} it follows that the hole current (majority carrier current) which flows through the back contact can be written as:

$$J_p(L_c) = -J_c(e^{-(qV_c/kT)} - 1), \quad (3)$$

where J_c stands for the contact saturation current (the voltage V_c is a reverse voltage for the contact). In the case of a drift and diffusion limited transport, J_c weakly depends on V_c . Equation (3) is valid if recombination in the contact space charge layer is negligible. This will be assumed throughout this paper.

A. Roll over

The total current of the solar cell is given by:

$$J = J_p(L_c) + J_n(L_c). \quad (4)$$

^{a)}Electronic mail: niemegee@elis.rug.ac.be

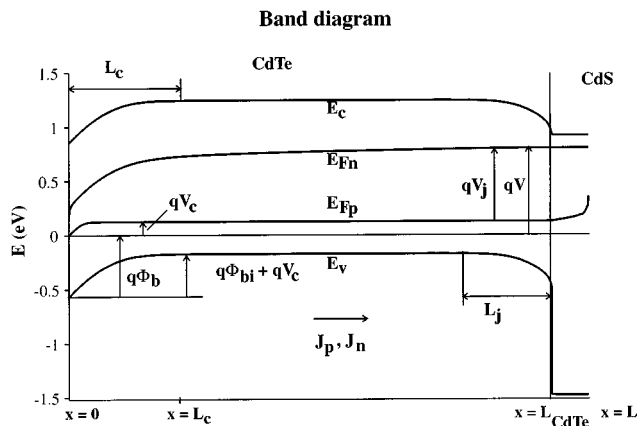


FIG. 1. Band diagram of a forward biased Au/CdTe/CdS solar cell with back contact barrier ($V = 0.8$ V, $q\Phi_b = 0.53$ eV).

The roll over of the IV curves occurs because the junction voltage saturates at high bias.³ This saturation occurs because of the back contact barrier and has nothing to do with the electron current at $x = L_c$: in this section, it is assumed that the total current equals the hole current at $x = L_c$. In the next section, the effect of a non-negligible electron current $J_n(L_c)$ will be discussed.

The dc characteristics of a solar cell with a back contact barrier can be modelled by a series connection of two diodes, with diode equations (2) and (3) (Fig. 2). The system of equations (1), (2) and (3) has been solved with MATHCAD for the case of a drift and diffusion limited back contact. The contact voltage and the junction voltage are shown in Fig. 3, as a function of applied bias for the dark and illuminated case. The total current is shown in Fig. 4 (curves 1dark and 1light). From (2) and (3) it follows that the saturation value of the junction voltage V_j , for a positive bias voltage V , in the dark is given by

$$V_{s\text{dark}} \approx \frac{nkT}{q} \ln \left(\frac{J_c}{J_s} \right) \quad (5)$$

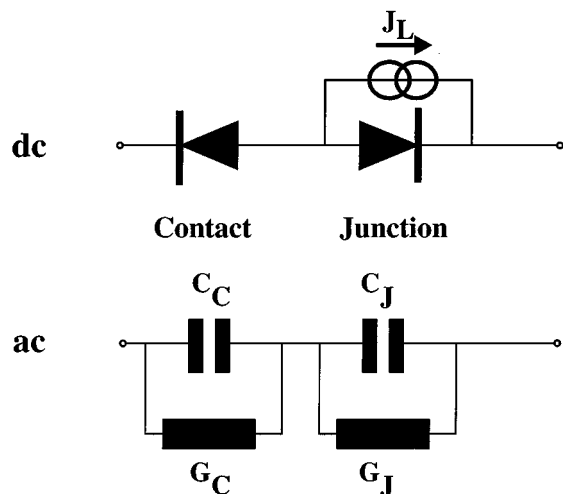


FIG. 2. Simple equivalent electrical circuit of the solar cell in dc and ac.

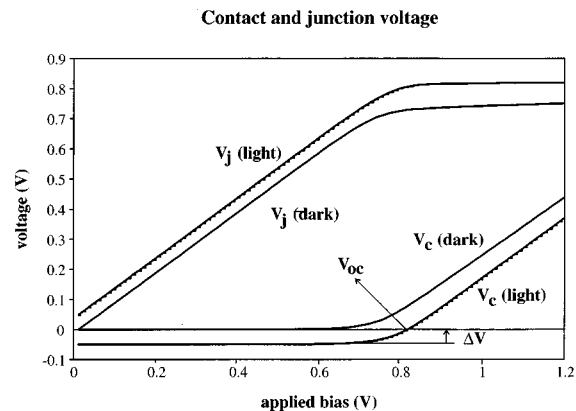


FIG. 3. Junction voltage V_j and contact voltage V_c as a function of applied bias, in the dark and under illumination, calculated with Eqs. (1), (2) and (3).

and the total current saturates at the contact saturation current J_c , i.e., roll over occurs. Under illumination, the junction voltage saturates at a higher value:

$$V_{s\text{light}} \approx V_{s\text{dark}} + \frac{nkT}{q} \ln \left(1 + \frac{J_L}{J_c} \right) \quad (6)$$

and the current also saturates at J_c . The assumptions made in this section will be referred to as “the simple model of Section II A.”

B. Cross over

In contrast with the previous section, we assume here that the electron current $J_n(L_c)$ is not negligible. We will show here that this current, which is the surface recombination current of electrons at the metal surface, may be responsible for the cross over of the IV curves.

We assume that the electron quasi-fermi level remains flat throughout the CdTe/CdS space charge layer and quasi-neutral regions: thus $E_{Fn}(L_c) - E_{Fp}(L_c) = qV_j$. This approximation is adequate if the CdTe diffusion length is sufficiently long in comparison with the thickness of the CdTe quasi-neutral region. For too short diffusion lengths, the ex-

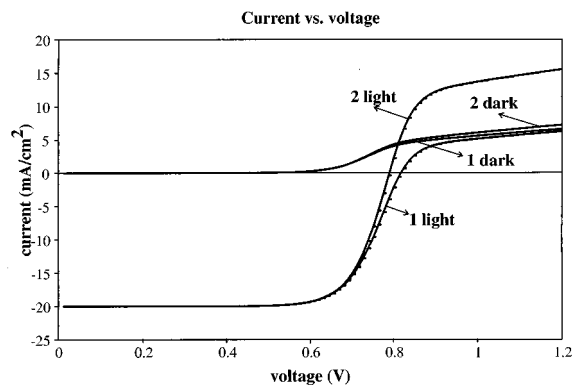


FIG. 4. Total current in the dark and under illumination, with the electron current $J_n(L_c)$ neglected [curves 1dark and 1light, Eqs. (1), (2) and (3)], and without neglecting $J_n(L_c)$ [curves 2dark and 2light, Eq. (9)].

cess electron concentration at the edge of the contact space charge layer is too small to cause any significant effect on the IV curves.

Neglecting recombination in the contact space charge layer, $J_n(x)$ is constant throughout this layer and given by the transport equation:

$$J_n = qD_n N_c e^{-[E_c(x)/kT]} \frac{d}{dx} e^{[E_{Fn}(x)/kT]} \quad (7)$$

with D_n the electron diffusion coefficient, N_c the conduction band effective density of states and $E_c(x)$ the conduction band energy at x . The traditional boundary condition for surface recombination reads:

$$J_n(L_c) = J_n(0) = qS_n[n(0) - n_0], \quad (8)$$

where S_n is the electron surface recombination velocity, $n(0)$ the electron concentration at $x=0$ and n_0 the equilibrium electron concentration at $x=0$. The electron current is calculated with a technique, commonly used to calculate the majority carrier current of a Schottky contact:⁷ integration of (7) between $x=0$ and $x=L_c$, together with the boundary condition (8), gives:

$$J_n(L_c) = qS_n \frac{n_i^2}{N_A} \frac{e^{qV_j/kT} - e^{-(qV_c/kT)}}{\frac{S_n L_d}{D_n} + e^{-[q(\Phi_{bi} + V_c)/kT]}}, \quad (9)$$

where n_i is the CdTe intrinsic concentration, N_A the CdTe acceptor concentration in the vicinity of the back contact and L_d is proportional to the extrinsic Debye length and given by $\sqrt{\pi\epsilon_s kT/2q^2 N_A}$, where ϵ_s is the CdTe permittivity. For realistic materials parameters and a sufficiently high contact potential $q\Phi_{bi}$, the term in S_n dominates the denominator of Eq. (9); one then obtains:

$$J_n(L_c) = q \frac{D_n}{L_d} \frac{n_i^2}{N_A} (e^{qV_j/kT} - e^{-(qV_c/kT)}) \quad (10)$$

$$\stackrel{\Delta}{=} J_{nsc} (e^{qV_j/kT} - e^{-(qV_c/kT)})$$

which is independent on the surface recombination velocity S_n .

As mentioned in Section II A, the junction voltage V_j saturates for high forward bias, and the saturation value is higher under illumination than in the dark [Eqs. (5) and (6)]. This means that, at high forward bias, the electron surface recombination current $J_n(L_c)$ saturates and is higher under illumination than in the dark (the term $e^{-(qV_c/kT)}$ in (10) becomes negligible at high forward bias). The hole current $J_p(L_c)$ is the same as in Section II A and saturates at J_c , independent of the illumination conditions. This means that the total current under illumination saturates at a higher value than the dark current. This is a possible explanation of the crossing of the dark and illuminated IV curves (Fig. 4, curves 2dark and 2light).

C. Fill factor loss

The simple model of Section II A allows us to investigate to what extent the presence of a back contact diode

influences the solar cell efficiency. To do so, we derived an approximate relationship between the solar cell efficiency and the saturation current J_c of the back contact diode (we neglect other sources of series resistance, and shunt resistance).

If we neglect the electron recombination current $J_n(L_c)$, the contact barrier plays the role of a series resistance and does not influence the cell open circuit voltage V_{oc} . Except for extremely high barrier heights, also the short circuit current of the solar cell is not affected by the presence of the contact diode. Hence, the total cell efficiency depends on the properties of the back contact only through the fill factor.

For an ideal solar cell (i.e., without series/shunt resistance or back contact barrier), the fill factor FF_0 is a function of the open circuit voltage only (to be precise: the open circuit voltage normalized to nkT/q), and this function only weakly depends on V_{oc} .⁸ Now consider the solar cell under short circuit conditions. The light current flows through the back contact as a forward majority carrier current. The back diode is then forward biased. From Eq. (3), it follows:

$$-V_c = \Delta V = \frac{kT}{q} \ln \left(1 + \frac{J_L}{J_c} \right).$$

Because the total device voltage equals zero at short circuit conditions, the opposite voltage drops over the junction. This means that a forward bias ΔV stands over the junction. For voltages below the maximum power point, the total device current can be considered constant, and therefore, also the voltage drop over the back contact diode remains constant (also see Fig. 3). Hence, in the fourth quadrant, the current-voltage characteristics in the presence of a back contact diode (non ideal IV curve) can be approximated by a translation of the ideal IV curve (i.e., with same V_{oc} and junction diode equation but with an ohmic back contact) over an amount ΔV , *except* for voltages around the open circuit voltage. If the non ideal IV curve were a translation of the *whole* ideal IV curve, the non ideal fill factor FF would approximate the fill factor of an ideal solar cell with open circuit voltage $V_{oc} - \Delta V$ (FF_0). Because the open circuit voltage of the non ideal cell is V_{oc} and not $V_{oc} - \Delta V$, the non ideal fill factor FF is given by:

$$FF \approx FF_0(v'_{oc}) \left[1 - \frac{kT}{qV_{oc}} \ln \left(1 + \frac{J_L}{J_c} \right) \right] \quad (11)$$

with FF_0 given by:⁸

$$FF_0(v'_{oc}) \approx \left(1 - \frac{\ln v'_{oc}}{v'_{oc}} \right) \left(1 - \frac{1}{v'_{oc}} \right) \frac{1}{1 - \exp(-v'_{oc})}$$

and where $v'_{oc} = q(V_{oc} - \Delta V)/nkT$. The function $FF_0(v'_{oc})$ is a slowly varying function of v'_{oc} . Fig. 5 shows the non ideal fill factor as a function of J_c , calculated with the simple model of Section II A (with constant J_L , and $V_{oc} = 0.7, 0.8$ and 0.9 eV), and the approximation (11) is shown for $V_{oc} = 0.9$ eV.

Regarding Eq. (11), it is now possible to define a “good” back contact: as long as the back diode saturation current J_c is larger than or equal to the light current, the fill

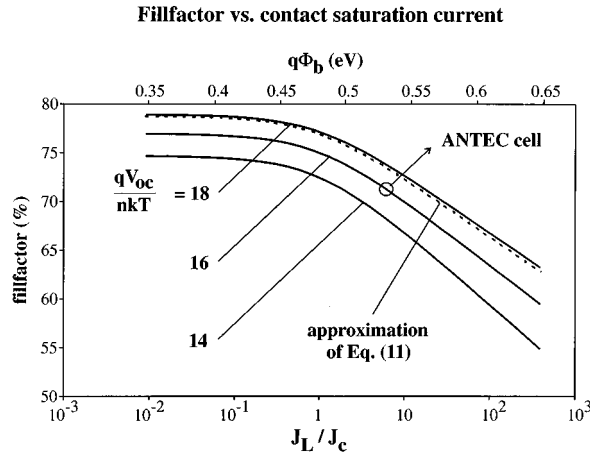


FIG. 5. Fill factor calculated with the simple model of Section II A, as a function of the contact saturation current J_c (barrier height $q\Phi_b$), for constant short circuit current J_L , and for an open circuit voltage of 0.7, 0.8, and 0.9 V (diode ideality factor = 2). The ANTEC cell has $V_{oc} = 0.8$ V and $q\Phi_b = 0.53$ eV. The approximation of Eq. (11) is shown for $V_{oc} = 0.9$ eV.

factor loss due to the back contact is only a few percent (depending on V_{oc}). Considerable fill factor loss occurs if the saturation current J_c is some orders of magnitude smaller than the light current J_L . In the practical case of a CdTe cell, the contact barrier height should not exceed 0.55 eV.

D. Capacitance vs voltage behaviour

In the following, capacitance denotes the imaginary part of the complex admittance divided by the pulsation ω , and conductance denotes the real part of the admittance. The small signal response of the solar cell is modelled by the equivalent electrical circuit of Fig. 2. This ac equivalent scheme is the series connection of the equivalent circuits of the junction and the Schottky diode. The individual diodes are modelled by a parallel connection of a diode capacitance and conductance. We assume that the frequency of the ac signal is low enough for the contact and junction conductances (G_c resp. G_j) to have their dc values:

$$G_c = \frac{qJ_c}{kT} e^{-(qV_c/kT)}$$

$$G_j = \frac{qJ_s}{nkT} e^{qV_j/nkT}.$$

The capacitance and conductance depend on the applied dc bias through the bias dependence of V_c and V_j . Using the values of V_c and V_j , calculated in Section II A, the total capacitance is calculated as a function of voltage (Fig. 6).

The presence of a back contact diode causes the CV curves to deviate from their expected monotonous behaviour: one can see that at low forward bias, the total capacitance increases with voltage. It subsequently goes through a maximum, quickly drops and goes through a second maximum again. Beyond this second maximum, the capacitance slowly decreases with voltage.

This behaviour is explained as follows:

(i) At low forward bias, the current is much smaller than the contact saturation current: therefore, there is no voltage

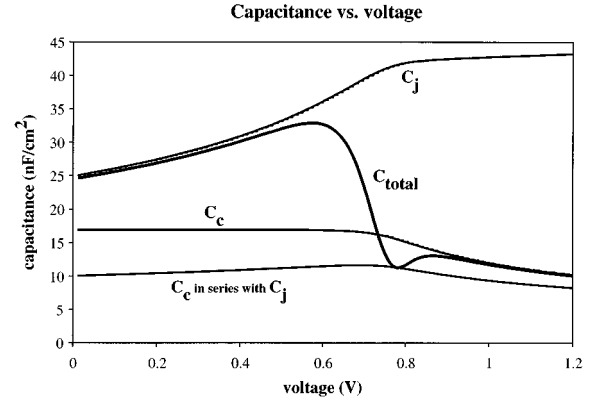


FIG. 6. Junction capacitance C_j , contact capacitance C_c , series connection of C_j and C_c , and the total capacitance as a function of applied bias, calculated with the simple model of Sections II A and II D (at 100 kHz).

drop over the contact; the applied dc bias totally drops over the CdS/CdTe junction, and so does the ac voltage (also see Figure 3). Consequently, the total capacitance equals the junction capacitance C_j at low bias: it increases with voltage and the slope of the $1/C(V)^2$ curve is determined by the CdTe doping profile in the vicinity of the CdS/CdTe junction.

(ii) At high voltage, the current is limited to the saturation current J_c of the contact and the junction voltage V_j saturates. All additional voltage drops over the contact (Fig. 3), so that now the applied ac voltage drops over the contact diode and the total capacitance equals the contact capacitance C_c . It decreases with increasing applied dc bias. The slope of the $1/C(V)^2$ curve is determined by the CdTe doping profile in the vicinity of the Au/CdTe back contact.

(iii) At intermediate voltages, the applied voltage is divided between the CdS/CdTe junction and the Au/CdTe contact. The total capacitance in this voltage region approximates the series connection of C_j and C_c , which is smaller than either of the two capacitances. If the width of the intermediate voltage region is not too narrow, the measured CV curve will thus exhibit a minimum between the two maxima, as the capacitance varies from C_j over $C_j C_c / (C_j + C_c)$ to C_c (Fig. 6).

III. MEASUREMENT

The above theoretical consideration were used to characterize in detail the Au/CdTe back contact in the Au/CdTe/CdS/TCO cell structure (supplied by ANTEC, Germany⁴).

Figure 7 shows the dark IV curves for different temperatures, measured in ELIS, Gent. Beyond the roll over point (i.e., when the current saturates), the IV curves show a small slope which decreases exponentially with temperature. This cannot be explained by thermionic emission, unless one assumes that the contact is shunted by a temperature dependent conductance. The assumption of a contact current which is limited by drift and diffusion is consistent with these measured data: in this case, J_c is given by $q\mu_p E(0)N_v e^{-(q\Phi_b/kT)}$. The small slope occurs because the electric field $E(0)$ depends on V_c , which depends on the applied bias, and also the temperature dependence of the

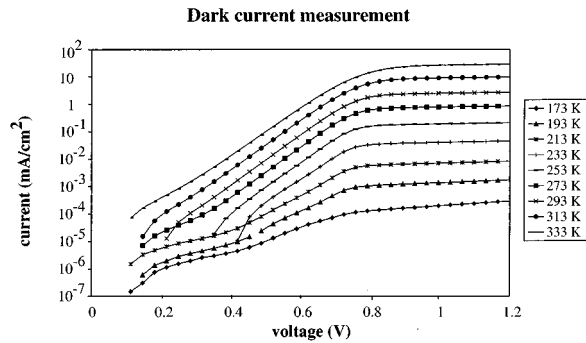


FIG. 7. Measured $I(V)$ curves at different temperatures of a CdS/CdTe cell supplied by ANTEC.

slope of the IV curve is obvious. The measured current depends on temperature as $T^{1/2}e^{-(q\Phi_b/kT)}$, with a barrier height $q\Phi_b$ of 0.53 eV. This is in agreement with a drift and diffusion limited current if one assumes that the CdTe hole mobility $\mu_p \sim 1/T$ in the measured temperature range. This corresponds with CdTe data from literature (mobility for polar optical scattering).⁹ This temperature dependence of J_c cannot be explained by thermionic emission, for which $J_c \sim T^2 e^{-(q\Phi_b/kT)}$. The IV curves for different illumination intensities (at room temperature) are shown in Fig. 8. The cross over could be explained by the surface recombination of electrons at the metal/semiconductor surface as explained in Section II B. Figure 9 shows a fully numerical simulation carried out by SCAPS-1D (see Section IV). Sometimes, it is argued that the cross over effect originates from a photovoltaic back contact. However, in the present case, generation of electron hole pairs in the contact space charge layer is negligible because of the thick CdTe layer ($\sim 10 \mu\text{m}$, CdTe deposited by CSS). Free carrier absorption (at long wavelengths) cannot explain the cross over either, because of the low CdTe doping concentration $\ll 10^{17}/\text{cm}^3$.¹⁰ Other explanations for the measured cross over are possible (e.g., charge from deep impurity levels in the vicinity of the contact may be excited to the conduction or valence band by the incident light). More experiments will be carried out in order to fur-

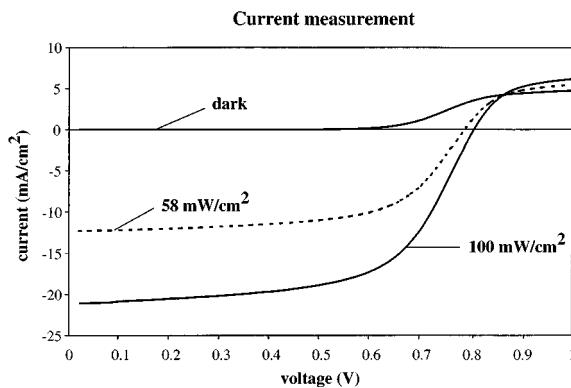


FIG. 8. Measured $I(V)$ curves at different intensities of the incident AM1.5G spectrum.

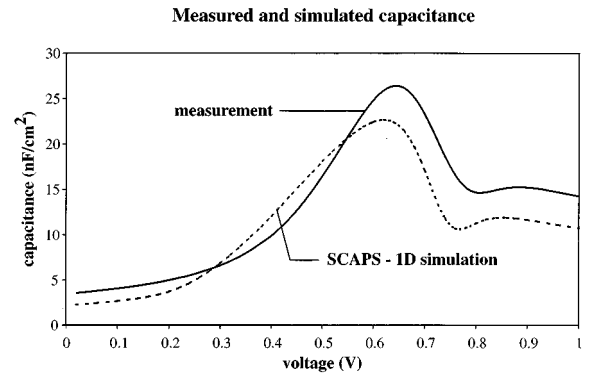


FIG. 9. Comparison of a capacitance vs voltage measurement in the dark (of an ANTEC cell) with a SCAPS-1D simulation (frequency=100 kHz; parameters listed in Table 1).

ther verify the applicability of the presented theory to the ANTEC cell.

The IV characteristics, measured under full AM1.5G illumination (i.e., $100 \text{ mW}/\text{cm}^2$), have a fill factor of 60%. An ideal solar cell, with a diode ideality factor n of 2 and an open circuit voltage of 800 mV has a fill factor of 77%. In Fig. 5, a back contact barrier for which $J_L/J_c \approx 5$ causes a fill factor loss of about 6%. The remainder of the fill factor loss can be attributed to the CdTe bulk series resistance, external series resistance and a voltage dependent current collection (these effects are not accounted for in the simple model, used to calculate Fig. 5). The fully numerical model (Section IV) does account for the series resistance of the CdTe bulk: the IV curve of Fig. 9, calculated numerically, has a fill factor of 66%.

The measured CV curve (Fig. 10) shows the features mentioned in Section II C. The CdTe doping profile in the junction region has been derived from the $1/C(V)^2$ curve at low forward bias, the doping concentration in the vicinity of the contact has been derived from the capacitance data at high forward bias. These values are listed in Table I, and serve as input for the fully numerical calculations (Section IV).

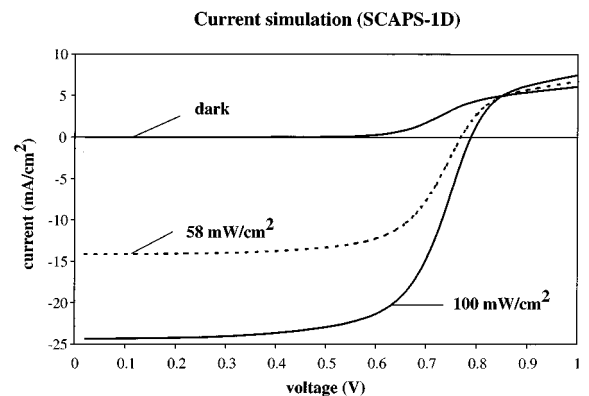


FIG. 10. SCAPS-1D simulation of the current-voltage characteristics, to be compared with the measurement of Fig. 8 (same simulation parameters as in Fig. 10).

TABLE I. Simulation parameters, used for the SCAPS-1D simulations. The symbols μ and τ stand for mobility resp. lifetime.

Layer	CdTe	CdTe	CdTe	Cds
thickness (μm)	1	13	0.5	1
type	p	p	p	n
$ N_A - N_D $ (/cm ³)	10^{15}	$2 \cdot 10^{13}$	see text	10^{17}
μ_n (cm ² /Vs)	10	100	100	100
μ_p (cm ² /Vs)	100	100	100	100
τ_n (s)	10^{-6}	10^{-6}	10^{-9}	10^{-8}
τ_p	10^{-6}	10^{-6}	10^{-9}	10^{-8}

The values of the CdTe doping concentration suggest that the CdS/CdTe interface is n^+p type. Elsewhere,^{11,12} we have shown that in the case of an n^+p type junction, recombination in the absorber space charge layer dominates over interface recombination. The assumption that space charge layer recombination dominates the junction transport is corroborated by the fact that the diode ideality factor of the junction current (low voltage part of Fig. 7) approaches 2 (at room temperature).

IV. FULLY NUMERICAL CALCULATIONS

At the University of Gent, the fully numerical program SCAPS-1D (a solar cell capacitance simulator in one dimension⁵) has been developed in order to improve our understanding of admittance measurements on thin film heterojunction solar cells. SCAPS-1D calculates dc and ac characteristics for a wide variety of semiconductor structures. It has been applied here to the ANTEC cell structure to simulate roll over, cross over and the capacitance-voltage characteristics. Figure 10 shows the IV curves for different intensities of the incident AM1.5G spectrum, and Fig. 9 shows the capacitance. For both calculations, the parameters of Table I have been used. As can be read from Table I, we assume that the CdTe layer at the back contact has a higher doping concentration than the bulk CdTe. This value of the doping concentration is derived from the slope $1/C(V)^2$ curve at high forward bias. The smaller value of μ_n in the contact layer fits the different saturation values of the IV curves of Fig. 8. Also the CdTe in the vicinity of the CdS/CdTe junction is assumed to differ from the bulk layer. It is assumed that this layer has an acceptor concentration at the metallurgical junction of $2 \cdot 10^{16}$ /cm³, decreasing exponentially toward the CdTe bulk with a characteristic length of $0.15 \mu\text{m}$ (not shown in Table I). This doping profile has been derived from the slope of the measured $1/C(V)^2$ curve at low forward voltages. Further, it is assumed that all recombination takes place in the vicinity of the metallurgical junction (i.e., in the

CdTe space charge layer; the CdTe has been deposited by CSS onto CdS). The carrier lifetimes of this interface layer fit the measured open circuit voltage. Finally, a barrier height $q\Phi_b$ of 0.53 eV fits the saturation current.

V. CONCLUSIONS

Transport through the Au/CdTe back contact is limited by drift and diffusion. The presence of a Schottky barrier causes roll over of the IV curves. We showed that cross over in CdTe cells may be caused by surface recombination of electrons at the back contact. Also related with the back contact barrier is the peculiar behaviour of the capacitance-voltage curves: we showed that beyond the roll over point, the contact capacitance is measured, so that it is possible to deduce the doping concentration in the vicinity of the back contact by capacitance measurements on the whole cell. A new, practical definition of a good back contact has been given, using an approximate relationship between the fill factor of a solar cell and the saturation current of the back contact.

ACKNOWLEDGMENTS

We acknowledge ANTEC for the supply of the CdS/CdTe cells, the Flemish FWO (M. Burgelman, research associate) and the Flemish IWT (A. Niemegeers, research engineer).

¹J. Britt and C. Ferekides, Appl. Phys. Lett. **62**, 2851 (1993).

²T. Chu and S. Chu, Prog. Photovolt. **1**, 31 (1993).

³G. Stollwerck and J. R. Sites, "Analysis of CdTe Back-Contact Barriers," Proceedings of the 13th European Photovoltaic Solar Energy Conference, Nice, 1995, p. 2020.

⁴D. Bonnet, H. Richter, and K.-H. Jäger, "The CTS Thin Film Solar Module—Closer to Production," Proceedings of the 13th European Photovoltaic Solar Energy Conference, Nice, 1995, p. 1456.

⁵A. Niemegeers and M. Burgelman, "Numerical modelling of ac-characteristics of CdTe and CIS solar cells," presented at the 25th IEEE Photovoltaic Specialists Conference, Washington D.C., May 1996.

⁶S. Sze, *Physics of Semiconductor Devices*, 2nd. ed. (Wiley, New York, 1981), p. 245.

⁷E. H. Rhoderick, *Metal-Semiconductor Contacts* (Clarendon, Oxford, 1978), p. 77.

⁸A. De Vos, Sol. Cells **8**, 286 (1983).

⁹Landolt-Börnstein, "Numerical Data and Functional Relationships in Science and Technology," *New Series* (Springer, Berlin, 1982), Vol. 17, subvol. b, p. 459.

¹⁰D. K. Schroder, *Semiconductor Material and Device Characterization* (Wiley, New York, 1990), p. 387.

¹¹M. Burgelman, A. De Vos and A. Niemegeers, "Device simulation of polycrystalline heterojunction solar cells," Proceedings of the 12th European Photovoltaic Solar Energy Conference, Amsterdam, 1994, p. 1557.

¹²A. Niemegeers, M. Burgelman, and A. De Vos, Appl. Phys. Lett. **67**, 843 (1995).